

Quasiparticle nature of rotational bands in ^{185}Pt

S. Pilotte, G. Kajrys, and S. Monaro

Laboratoire de Physique Nucléaire, Université de Montréal, Montréal, Québec, Canada H3C 3J7

M. P. Carpenter,* V. P. Janzen,† and L. L. Riedinger

Department of Physics, University of Tennessee, Knoxville, Tennessee 37996

J. K. Johansson, D. G. Popescu,‡ D. D. Rajnauth, and J. C. Waddington

Tandem Accelerator Laboratory, Department of Physics, McMaster University, Hamilton, Ontario, Canada L8S 4K1

(Received 9 January 1989)

High-spin states in ^{185}Pt have been studied with the $^{173}\text{Yb}(^{16}\text{O},4n)^{185}\text{Pt}$ reaction at 90 MeV using a multidetector array consisting of five Ge detectors and a multiplicity filter of six NaI counters. Rotational bands built on the Nilsson configurations $\frac{9}{2}^+[624]$, $\frac{7}{2}^-[503]$, and $\frac{1}{2}^-[521]$ have been identified and interpreted within the framework of the cranked shell model. Additional band structures built on levels at 3.131 and 3.294 MeV are observed which arise from more complex configurations. Experimental values of $B(M1;I \rightarrow I-1)/B(E2;I \rightarrow I-2)$ ratios have been extracted and compared to predictions of the semiclassical Döna and Frauendorf approach.

I. INTRODUCTION

The Pt-Hg nuclei at the upper limit of the rare-earth region are known to exhibit shape coexistence phenomena. This behavior has been predicted and is well documented.¹⁻⁸ The Hg nuclei^{9,10} have an oblate ground state and low-lying prolate structures for $189 > A > 177$. However, the Pt nuclei have a more transitional character starting with well-deformed prolate shapes for $182 > A > 176$ to oblate shapes for the heavier isotopes ($A \geq 192$). One also expects these soft nuclei to be easily deformed via a polarization effect arising from valence nucleons or quasiparticles associated with band crossings.

The $^{184-185}\text{Pt}$ nuclei are particularly interesting since both a prolate ground state and an excited oblate structure have been reported in ^{185}Au (Ref. 11) and ^{186}Pt (Ref. 12). Extensive knowledge of low-spin levels in ^{185}Pt is provided from decay studies of Au isotopes,¹³⁻¹⁵ but few studies have focused on high-spin states.¹⁶⁻¹⁸ As part of a systematic study of the $^{182-188}\text{Pt}$ isotopes, the structure of high-spin states in ^{185}Pt has been determined. The nature of the different crossings is investigated by looking at the $B(M1)/B(E2)$ ratios and experimental Routhians.

II. EXPERIMENTAL DETAILS

The ^{16}O beam from the McMaster tandem accelerator was used to bombard an isotopically enriched target of ^{173}Yb (1 mg cm^{-2}) on a Pb foil backing to stop the recoil nuclei. At a bombarding energy of 90 MeV the $(^{16}\text{O},4n)$ reaction channel populates strongly ($\sim 50\%$ of the total evaporation yield) high-spin states in ^{185}Pt , bringing in some $36\hbar$ of angular momentum. Deexcitation γ rays were detected by an array of five Ge detectors and six NaI counters, the latter acting as a multiplicity filter. Energy resolution and efficiency of the germanium detectors were 2.2 keV (1.173 MeV transition from ^{60}Co) and

24%, respectively. Coincidences consisting of three Ge detectors or two Ge detectors plus two NaI counters firing were recorded event by event onto magnetic tape for subsequent analysis. Some 100×10^6 γ - γ coincidences were collected and sorted into a 4096×4096 matrix from which background was subtracted. The decay scheme was constructed from gates set on about 250 transitions appearing in the total spectrum. Some examples of the coincidence spectra are shown in Fig. 1.

Angular distributions were measured simultaneously by the five Ge detectors, which were placed at -10° , 30° , 45° , 60° , and 90° to the beam direction with the condition that one Ge detector and two NaI counters fired. Detector efficiencies were determined with a standard ^{152}Eu source placed at the target location. Peak areas were obtained with the peak fitting code SAMPO,¹⁹ and the angular distributions were analyzed with the computer code THAD (theoretical angular distribution²⁰) to extract the experimental A_0 , A_2 , and A_4 coefficients. For mixed transitions the mixing ratio δ was obtained following the procedures of Rose and Brink.²¹

III. RESULTS AND DISCUSSION

A summary of the level energies, transition energies, relative intensities, and angular distribution results is presented in Table I, while the decay scheme is shown in Fig. 2.

A previous study¹⁸ had already established bands 1 and 2 up to the $\frac{25}{2}^+$, 1417.4 keV level while more recent decay work^{15,22} determined the low-lying structure of both positive- and negative-parity levels. Bands 3 and 4 are built on the known $\frac{7}{2}^-$ level at 310.4 keV. Our angular distribution measurements of the 176.1 and 195.2 keV γ rays strongly support $\Delta I = 1$ character. A complete set of crossover and cascade transitions forms this strongly coupled band. These results are in agreement with the

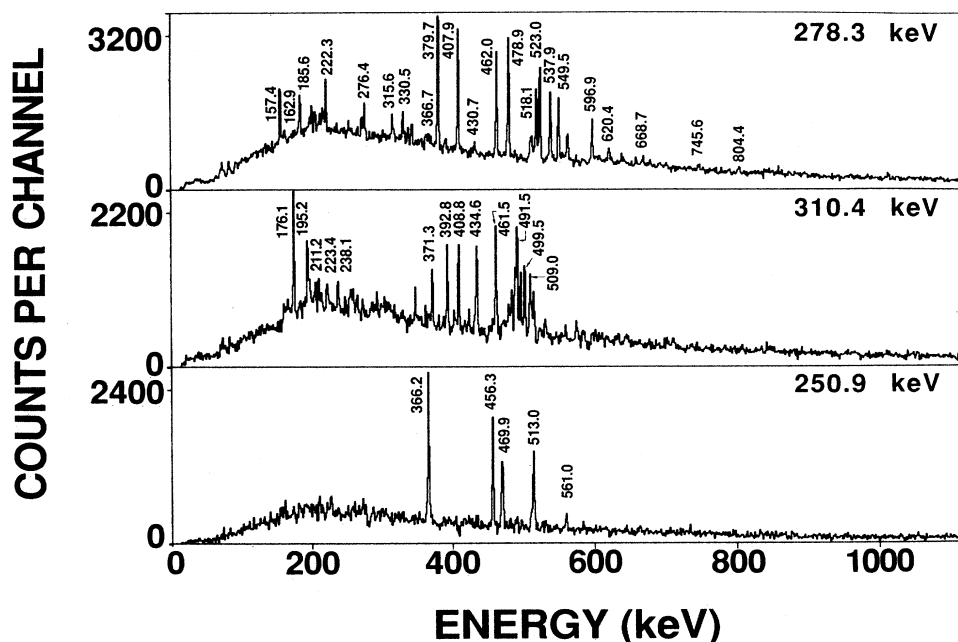


FIG. 1. Some typical examples of the γ - γ coincidence spectra observed in the $^{173}\text{Yb}(^{16}\text{O}, 4n)^{185}\text{Pt}$ reaction. The labeled peaks belong to ^{185}Pt and all energies are in keV. Note that no background correction was applied.

most recent assignments of Roussière *et al.*²² Placement of band 5, built on the $\frac{1}{2}^-$ level at 103 keV, relies on the identification of the 250.9 keV $E2$ γ ray reported in decay work. Note that the 97.0 keV $\frac{5}{2}^- \rightarrow \frac{1}{2}^-$ transition has not been observed in this work but has been placed in

the level scheme for completeness. Two additional bands (6 and 7) are based on the $(\frac{33}{2}^-)$ 3131.4 keV and $(\frac{35}{2}^-)$ 3294.3 keV levels, respectively. The spin assignments are based on the angular distributions of the transitions decaying to the yrast band, which are compatible with

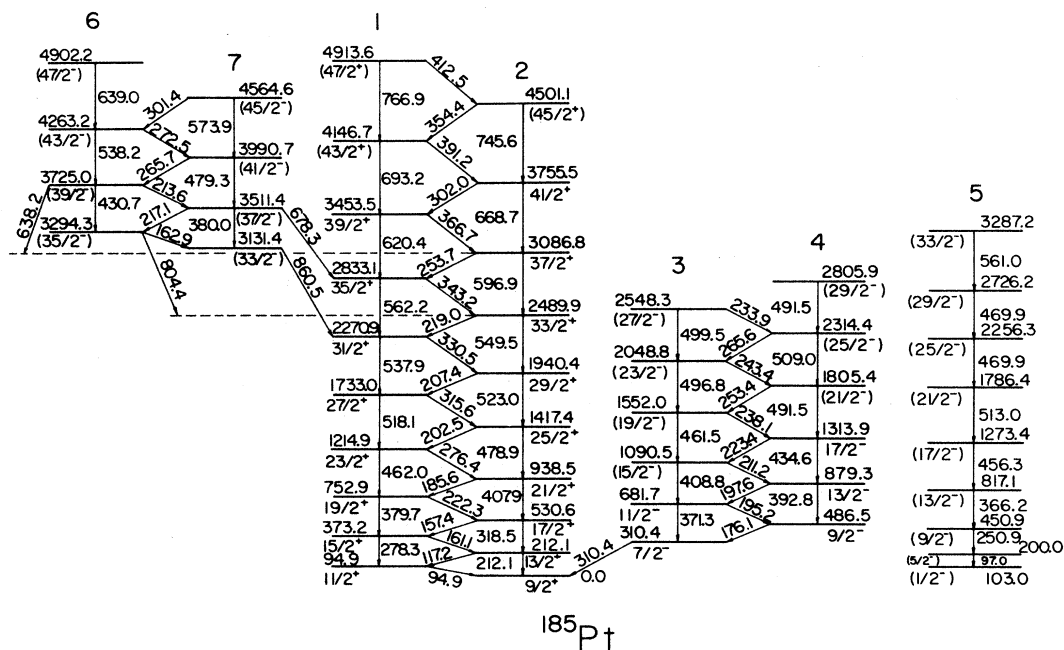


FIG. 2. The decay scheme of ^{185}Pt obtained in this work. Strongly connected levels have been grouped together into bands 1-7 and all energies are in keV. Spins in parentheses are considered probable but not definitely established.

TABLE I. Transitions in ^{185}Pt .

Transition (keV)	Level (keV)	J_i^π	J_f^π	I_γ (%)	A_2/A_0	A_4/A_0	Multipolarity ^a
94.9	94.9	$\frac{11}{2}^+$	$\frac{9}{2}^+$				
117.2	212.1	$\frac{13}{2}^+$	$\frac{11}{2}^+$	19.7(9)	-0.68(7)	-0.01(5)	0.30(7)
157.4	530.6	$\frac{17}{2}^+$	$\frac{15}{2}^+$	18.3(7)	-0.70(6)	0.08(4)	0.28(6)
161.1	373.2	$\frac{15}{2}^+$	$\frac{13}{2}^+$	30.1(21)	-0.77(6)	0.10(8)	0.30(7)
162.9	3294.3	$(\frac{35}{2}^-)$	$(\frac{33}{2}^-)$				
176.1	486.5	$\frac{9}{2}^-$	$\frac{7}{2}^-$	5.4(2)	-0.71(6)	0.05(4)	
185.6	938.5	$\frac{21}{2}^+$	$\frac{19}{2}^+$	12.6(7)	-0.67(8)	0.05(6)	0.26(8)
195.2	681.7	$\frac{11}{2}^-$	$\frac{9}{2}^-$	3.4(4)	-0.64(6)	-0.06(4)	
197.6	879.3	$\frac{13}{2}^-$	$\frac{11}{2}^-$	2.9(4)	-0.37(6)	0.02(5)	
202.5	1417.4	$\frac{25}{2}^+$	$\frac{23}{2}^+$	10.0(4)	-0.59(6)	0.10(4)	0.17(3)
207.4	1940.4	$\frac{29}{2}^+$	$\frac{27}{2}^+$	7.5(9)	-0.64(7)	0.11(6)	0.11(11)
211.2	1090.5	$(\frac{15}{2}^-)$	$\frac{13}{2}^-$				
212.1	212.1	$\frac{13}{2}^+$	$\frac{9}{2}^+$	10.5(9)	0.20(6)	-0.03(5)	E2
213.6	3725.0	$(\frac{39}{2}^-)$	$(\frac{37}{2}^-)$	5.3(2)	-0.44(5)	0.10(5)	
217.1	3511.4	$(\frac{37}{2}^-)$	$(\frac{35}{2}^-)$	4.7(3)	-0.35(5)	-0.05(5)	
219.0	2489.9	$\frac{33}{2}^+$	$\frac{31}{2}^+$	6.3(4)	-0.46(8)	-0.01(7)	0.18(8)
222.3	752.9	$\frac{19}{2}^+$	$\frac{17}{2}^+$	22.1(6)	-0.81(3)	0.12(2)	0.33(8)
223.4	1313.9	$\frac{17}{2}^-$	$(\frac{15}{2}^-)$				
233.9	2548.3	$(\frac{27}{2}^-)$	$(\frac{25}{2}^-)$				
238.1	1552.0	$(\frac{19}{2}^-)$	$(\frac{17}{2}^-)$				
243.4	2048.8	$(\frac{23}{2}^-)$	$(\frac{21}{2}^-)$				
250.9	450.9	$(\frac{9}{2}^-)$	$(\frac{5}{2}^-)$	11.0(4)	0.32(4)	-0.12(6)	E2
253.4	1805.4	$(\frac{21}{2}^-)$	$(\frac{19}{2}^-)$				
253.7	3086.8	$\frac{37}{2}^+$	$\frac{35}{2}^+$	4.3(2)	-0.50(7)	-0.03(5)	0.19(8)
265.6	2314.4	$(\frac{25}{2}^-)$	$(\frac{23}{2}^-)$				
265.7	3990.7	$(\frac{41}{2}^-)$	$(\frac{39}{2}^-)$	5.3(3)	-0.43(5)	0.12(5)	
272.5	4263.2	$(\frac{43}{2}^-)$	$(\frac{41}{2}^-)$				
276.4	1214.9	$\frac{23}{2}^+$	$\frac{21}{2}^+$	13.7(5)	-0.79(6)	0.13(4)	0.36(10)
278.3	373.2	$\frac{15}{2}^+$	$\frac{11}{2}^+$	30.2(45)	0.36(27)	-0.11(9)	E2
301.4	4564.6	$(\frac{45}{2}^-)$	$(\frac{43}{2}^-)$				
302.0	3755.5	$\frac{41}{2}^+$	$\frac{39}{2}^+$	4.0(2)	-0.51(7)	0.16(7)	0.13(8)
310.4	310.4	$\frac{7}{2}^-$	$\frac{9}{2}^+$	20.2(8) ^b	-0.89(5)	-0.01(5)	
315.6	1733.0	$\frac{27}{2}^+$	$\frac{25}{2}^+$	14.0(17)	-0.47(21)	0.10(19)	0.15(3)
318.5	530.6	$\frac{17}{2}^+$	$\frac{13}{2}^+$	52.5(11)	0.33(2)	-0.11(2)	E2
330.5	2270.9	$\frac{31}{2}^+$	$\frac{29}{2}^+$	13.3(9)	-0.67(11)	0.10(9)	0.27(8)
343.2	2833.1	$\frac{35}{2}^+$	$\frac{33}{2}^+$	10.7(4)	-0.61(6)	0.15(5)	0.19(8)
354.4	4501.1	$(\frac{45}{2}^+)$	$(\frac{43}{2}^+)$	2.7(4)			
366.2	817.1	$(\frac{13}{2}^-)$	$(\frac{9}{2}^-)$				
366.7	3453.5	$\frac{39}{2}^+$	$\frac{37}{2}^+$	7.3(4)	-0.30(8)	0.11(10)	0.10(8)
371.3	681.7	$\frac{11}{2}^-$	$\frac{7}{2}^-$	4.0(1)	0.36(5)	-0.16(7)	E2
379.7	752.9	$\frac{19}{2}^+$	$\frac{15}{2}^+$	52.9(11)	0.32(2)	-0.08(2)	E2
380.0	3511.4	$(\frac{37}{2}^-)$	$(\frac{35}{2}^-)$				
391.2	4146.7	$(\frac{43}{2}^+)$	$\frac{41}{2}^+$	3.8(4)			
392.8	879.3	$\frac{13}{2}^-$	$\frac{9}{2}^-$	8.2(3)	0.43(5)	-0.04(6)	E2
407.9	938.5	$\frac{21}{2}^+$	$\frac{17}{2}^+$	82.1(19)	0.33(2)	-0.08(2)	E2

TABLE I. (Continued).

Transition (keV)	Level (keV)	J_i^π	J_f^π	I_γ (%)	A_2/A_0	A_4/A_0	Multipolarity ^a
408.8	1090.5	$(\frac{15}{2}^-)$	$\frac{11}{2}^-$				
412.5	4913.6	$(\frac{47}{2}^+)$	$(\frac{45}{2}^+)$	2.9(9)			
430.7	3725.0	$(\frac{39}{2}^-)$	$(\frac{35}{2}^-)$	4.9(2)	0.53(5)	-0.06(6)	E2
434.6	1313.9	$\frac{17}{2}^-$	$\frac{13}{2}^-$	9.0(3)	0.32(5)	0.04(6)	E2
456.3	1273.4	$(\frac{17}{2}^-)$	$(\frac{13}{2}^-)$	13.4(5)	0.31(5)	-0.10(6)	E2
461.5	1552.0	$(\frac{19}{2}^-)$	$(\frac{15}{2}^-)$				
462.0	1214.9	$\frac{23}{2}^+$	$\frac{19}{2}^+$	57.1(20)	0.32(5)	-0.06(6)	E2
469.9	2256.3	$(\frac{25}{2}^-)$	$(\frac{21}{2}^-)$				
469.9	2726.2	$(\frac{29}{2}^-)$	$(\frac{25}{2}^-)$				
478.9	1417.4	$\frac{25}{2}^+$	$\frac{21}{2}^+$	100(3)	0.31(2)	-0.05(3)	E2
479.3	3990.7	$(\frac{41}{2}^-)$	$(\frac{37}{2}^-)$				
491.5	2805.9	$(\frac{29}{2}^-)$	$(\frac{25}{2}^-)$				
491.5	1805.4	$(\frac{21}{2}^-)$	$(\frac{17}{2}^-)$				
496.8	2048.8	$(\frac{23}{2}^-)$	$(\frac{19}{2}^-)$				
499.5	2548.3	$(\frac{27}{2}^-)$	$(\frac{23}{2}^-)$				
509.0	2314.4	$(\frac{25}{2}^-)$	$(\frac{21}{2}^-)$				
513.0	1786.4	$(\frac{21}{2}^-)$	$(\frac{17}{2}^-)$				
518.1	1733.0	$\frac{27}{2}^+$	$\frac{23}{2}^+$	40.2(12)	0.36(3)	-0.09(4)	E2
523.0	1940.4	$\frac{29}{2}^+$	$\frac{25}{2}^+$	91.7(24)	0.30(2)	-0.05(3)	E2
537.9	2270.9	$\frac{31}{2}^+$	$\frac{27}{2}^+$	42.9(14)	0.31(5)	-0.03(6)	E2
538.2	4263.2	$(\frac{43}{2}^-)$	$(\frac{39}{2}^-)$				
549.5	2489.9	$\frac{33}{2}^+$	$\frac{29}{2}^+$	50.0(10)	0.30(2)	-0.04(3)	E2
561.0	3287.2	$(\frac{33}{2}^-)$	$(\frac{29}{2}^-)$				
562.2	2833.1	$\frac{35}{2}^+$	$\frac{31}{2}^+$	19.5(6)	0.26(4)	-0.03(4)	E2
573.9	4564.6	$(\frac{45}{2}^-)$	$(\frac{41}{2}^-)$	9.2(3)	0.28(5)	-0.04(5)	(E2)
596.9	3086.8	$\frac{37}{2}^+$	$\frac{33}{2}^+$	30.2(9)	0.24(3)	-0.04(3)	E2
620.4	3453.5	$\frac{39}{2}^+$	$\frac{35}{2}^+$	12.6(5)	0.24(6)	-0.04(6)	(E2)
638.2	3725.0	$(\frac{39}{2}^-)$	$\frac{37}{2}^+$				
639.0	4902.2	$(\frac{47}{2}^-)$	$(\frac{43}{2}^-)$				
668.7	3755.5	$\frac{41}{2}^+$	$\frac{37}{2}^+$	11.8(4)	0.14(4)	-0.02(4)	(E2)
678.3	3511.4	$(\frac{37}{2}^+)$	$\frac{35}{2}^+$	6.8(3)	-0.25(5)	0.08(5)	(E1)
693.2	4146.7	$(\frac{43}{2}^+)$	$\frac{39}{2}^+$	4.5(5)			
745.6	4501.1	$(\frac{45}{2}^+)$	$\frac{41}{2}^+$	3.9(4)			
766.9	4913.6	$(\frac{47}{2}^+)$	$(\frac{43}{2}^+)$	2.2(4)			
804.4	3294.3	$(\frac{35}{2}^-)$	$\frac{33}{2}^+$	6.9(3)	-0.41(6)	0.22(5)	(E1)
860.5	3131.4	$(\frac{33}{2}^-)$	$\frac{31}{2}^+$	7.0(3)	-0.29(6)	0.07(9)	(E1)

^aFor mixed transitions the measured $\delta(E2/M1)$ is given, following the sign convention of Rose and Brink (Ref. 21).

^bComposite line.

$\Delta I = 1$ transitions. The absence of any E2 transition between these two structures suggests that this structure and the yrast band have opposite parity (see also subsection A for a discussion of the configuration assignment).

Bands 1 and 2, which are strongly coupled, have been

extended in this work up to the $\frac{47}{2}^+$ state at 4913.6 keV. In the decay work¹⁵ a $\frac{3}{2}^-$ level at 180.8 keV and a $\frac{7}{2}^-$ level at 423.8 keV were strongly populated but were not observed in this study. A similar result has been obtained²³ in ^{183}Pt , where only the $\frac{1}{2}^-$ band could be identified.

A. Band assignments

A standard single-particle neutron level diagram shows that for a prolate deformed nucleus ($\beta_2=0.25$) the $\frac{9}{2}^+$ [624] and $\frac{7}{2}^+$ [633] orbitals will be important constituents of the positive-parity levels. For the negative-parity states the $\frac{7}{2}^-$ [503], $\frac{7}{2}^-$ [514], $\frac{5}{2}^-$ [512], and $\frac{1}{2}^-$ [521] orbitals lie close to the Fermi surface.

In the framework of the cranked shell model the rotational characteristics of band structures can be determined by calculating the aligned angular momentum (i) and energy in the rotating frame (the Routhian e') as a function of the rotational frequency ω in the usual manner.²⁴ Such a plot is shown in Fig. 3 for the observed quasiparticle configurations in ^{185}Pt , where the contributions from the rotating core have been subtracted as described in the figure caption. For ease of reference the quasiparticles have been labeled by letters as noted in the figure.

Bands 1 and 2 in ^{185}Pt can be identified as the two signatures²⁴ A ($\alpha=+\frac{1}{2}$) and B ($\alpha=-\frac{1}{2}$) of the $\frac{9}{2}^+$ [624] band structure originating from the $\nu i_{13/2}$ shell-model structure, as previously suggested.^{18,15} An initial alignment of $\approx 4.5\hbar$ at $\hbar\omega=0.2$ MeV, and a small amount of energy splitting between the two signatures are both consistent with a $K=\frac{9}{2}$ orbital from the $i_{13/2}$ subshell.

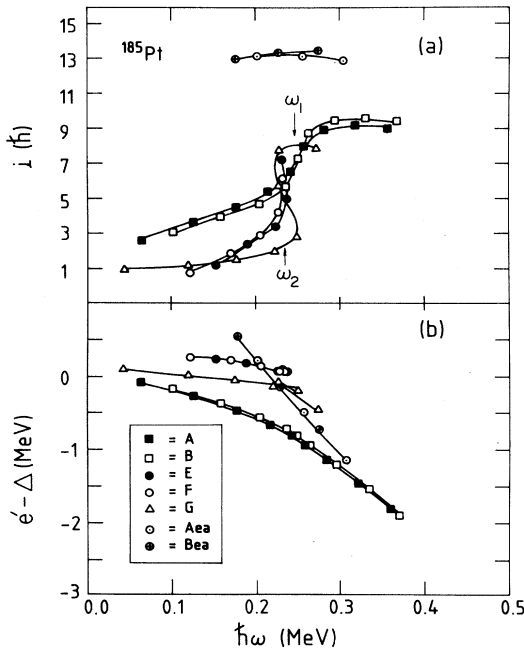


FIG. 3. The experimental aligned angular momenta i [part (a)] and Routhians e' [part (b)] vs rotational frequency, $\hbar\omega$, for bands in ^{185}Pt . The letters denote quasiparticle configurations of the following rotational signatures originating from the listed single-particle states and Nilsson orbitals. A and B , $\alpha=\frac{1}{2}$, and $\alpha=-\frac{1}{2}$, $\nu i_{13/2}$, $\frac{9}{2}^+$ [624]; E and F , $\alpha=\frac{1}{2}$ and $\alpha=-\frac{1}{2}$, $\nu f_{7/2}$, $\frac{7}{2}^-$ [503]; G , $\alpha=\frac{1}{2}$, $\nu p_{3/2}$, $\frac{1}{2}^-$ [521]; a , $\alpha=\frac{1}{2}$, $\pi i_{13/2}$, $\frac{1}{2}^+$ [660]; e , $\alpha=\frac{1}{2}$, $\pi h_{9/2}$, $\frac{1}{2}^-$ [541]. A reference due to the rotating core of $I_0=21.5\hbar^2 \text{ MeV}^{-1}$ and $I_1=100\hbar^3 \text{ MeV}^{-3}$ has been subtracted.

Bands 3 and 4 are interpreted as the two signatures E ($\alpha=-\frac{1}{2}$) and F ($\alpha=+\frac{1}{2}$) of the $\frac{7}{2}^-$ [503] structure. In this region there may be some mixing between the neutron $\Omega^\pi=\frac{7}{2}^-$ Nilsson states having asymptotic quantum numbers $\frac{7}{2}^-$ [514] and $\frac{7}{2}^-$ [503], and it is not clear that either the above designations or shell-model labels “ $f_{7/2}$ ” or “ $h_{9/2}$ ” are altogether valid. In terms of the rotational characteristics, the observed low initial alignment and the absence of any signature splitting are predicted for both “ $f_{7/2}$ ” and “ $h_{9/2}$ ” orbitals. Both the Woods-Saxon and Nilsson potentials predict the $\frac{7}{2}^-$ [514] configuration to be the lower of the two at $N=107$ (e.g., Ref. 24). However, from the decay of ^{185}Au Roussière *et al.*²² most recently assigned $\frac{7}{2}^-$ 310.4 keV, $\frac{9}{2}^-$ 486.5 keV, and $\frac{11}{2}^-$ 681.9 keV levels as members of the $\frac{7}{2}^-$ [503] band, contradicting previous¹⁵ spin-parity and configuration assignments. The $B(M1)/B(E2)$ measurement presented in Sec. III B confirms the $f_{7/2}$ $\frac{7}{2}^-$ [503] nature of this band.

As mentioned previously, band 5 is associated with the structure built on an isomeric $\frac{1}{2}^-$ state at 103 keV established in Ref. 15. There a $\frac{1}{2}^-$ [521] ($\nu p_{3/2}$ shell-model parentage) configuration was assigned to that band. This work extends the favored signature ($G, \alpha=\frac{1}{2}$) to the ($\frac{33}{2}^-$). Although the $\alpha=+\frac{1}{2}, I=\frac{3}{2}^-$ and $\frac{7}{2}^-$ states are populated in the previous decay study,¹⁵ the two partners are separated by a large degree of signature splitting, and in this work only the favored signature is observed. This large effect is consistent with a $K=\frac{1}{2}$ $\nu p_{3/2}$ configuration.

Bands 6 and 7 are clearly different from structures 1–5, originating at high spin and displaying a strikingly large amount of initial alignment (cf. Fig. 3). Only a three-quasiparticle configuration involving high- j orbitals could produce the observed $i \approx 13\hbar$. A very likely combination is the $\nu i_{13/2} \otimes \pi h_{9/2} \otimes \pi i_{13/2}$ configuration, in single-particle orbital notation $\nu \frac{9}{2}^+$ [624] $\otimes \pi \frac{1}{2}^-$ [541] $\otimes \pi \frac{1}{2}^+$ [660]. The $\nu i_{13/2}$ band, as already discussed, is yrast in this nucleus, while the two proton bands are lowest in the nearby ^{185}Au (Ref. 11) and ^{187}Au (Ref. 25) nuclei.

The two-quasiproton analog of the proposed structure has in fact been identified in the neighboring ^{184}Pt nucleus,²⁶ where a $\pi h_{9/2} \otimes \pi i_{13/2}$ band displays an initial alignment of $\approx 10\hbar$ at an energy $e'=0.81$ MeV above the yrast band at a frequency of 0.20 MeV. Using the additivity properties of both i and e' , the corresponding three-quasiparticle $\nu i_{13/2} \otimes \pi h_{9/2} \otimes \pi i_{13/2}$ structure in ^{185}Pt should have $i \approx 10\hbar + 4.5\hbar = 14.5\hbar$ and $e' \approx 0.81 \text{ MeV} + (-0.60 \text{ MeV}) = 0.21 \text{ MeV}$. This compares quite well to the observed values of $i \approx 13\hbar$ and $e' = 0.29 \text{ MeV}$.

Another possible candidate is the $\nu i_{13/2} \otimes \pi f_{7/2} \otimes \pi i_{13/2}$ combination, which based on the ^{185}Au Routhians¹¹ should lie slightly higher in energy than the configuration just discussed. However, it is clear that in ^{184}Pt the $\pi h_{9/2} \otimes \pi i_{13/2}$ configuration is preferred over the $\pi f_{7/2} \otimes \pi i_{13/2}$ combination, because only the total signature $\alpha=1$ component (odd spins) of the two-proton band is observed.²⁶ This can only arise from the $\pi h_{9/2}$ ($\alpha=+\frac{1}{2}$ highly favored) plus $\pi i_{13/2}$ ($\alpha=+\frac{1}{2}$ again highly

avored) coupling. The lowest signature of a $\pi f_{7/2} \otimes \pi i_{13/2}$ band would be $\alpha=0$ (even spins), since the favored signature of the $\pi f_{7/2}$ band is $\alpha=-\frac{1}{2}$ [cf. ^{185}Au (Ref. 11)].

B. $B(M1)/B(E2)$ measurements

Additional evidence as to the quasiparticle makeup of rotational bands can be gathered from measurements of the $B(M1; I \rightarrow I-1)/B(E2; I \rightarrow I-2)$ values. These ratios have been obtained from experimental $I_\gamma(\Delta I=2)/I_\gamma(\Delta I=1)$ branching ratios (λ) and $M1/E2$ mixing ratios (δ). For a theoretical description of the $B(M1)$ and $B(E2)$ matrix elements we turn to the semiclassical formalism of Dönau and Frauendorf.^{27,28} The predictions of this model are very sensitive to the quasiparticle configurations involved, primarily through the $g_K - g_R$, K , and alignment values. Of course the g factors themselves are extremely dependent on the quasiparticles considered, especially when comparing neutron and proton excitations. Because of the opposite signs of the proton versus neutron g factors, a mixed $\pi \otimes \nu$ configuration normally exhibits enhanced $M1$ transitions relative to a structure involving only a single quasiparticle.

The experimental $B(M1)/B(E2)$ ratios and theoretical predictions for ^{185}Pt are compared in Table II. Experimental values are from this work with the exception of the $\nu p_{3/2}$ configurations in ^{185}Pt and ^{183}Os , for which data are taken from the decay studies of Roussi re *et al.*^{15,22} For the theoretical parameters, we have used

g_K factors given by the Schmidt limits with $g_s=0.7g_s$ (free) as in Ref. 28 and $g_R=0.4$. K values are taken from the appropriate Nilsson configurations, i.e., $K=\frac{9}{2}$ ($\nu i_{13/2}$), $\frac{7}{2}$ ($\nu f_{7/2}$, $\nu h_{9/2}$), and $\frac{1}{2}$ ($\nu p_{3/2}$, $\pi h_{9/2}$, $\pi f_{7/2}$, $\pi i_{13/2}$). The alignment values are taken from experiment (see Fig. 3).

A complete set of measurements from the $\nu i_{13/2} \frac{9}{2}^+$ [624] band in ^{185}Pt has been presented in Ref. 29. As shown by the averaged results listed in Table II, the low-spin values are fairly well reproduced by the theory. At high spin the large experimental increase can only be explained by the alignment of a pair of $h_{9/2}$ protons (see also the following).

For the remainder of the bands experimental $B(M1)/B(E2)$ ratios are only available for isolated spins. However, the overall agreement based on those limited values is quite good. It appears that bands 3 and 4 are fairly accurately described as a $\nu f_{7/2}$ configuration versus a $\nu h_{9/2}$ structure. The particular comparison there is between orbitals having $l+s$ ($\nu f_{7/2}$) and $l-s$ ($\nu h_{9/2}$) spin-orbit coupling, since the K and i values are identical.

The experimental value for band 5 (and for the corresponding band in ^{183}Os) is very much smaller than any of the other measurements. This is reflected in the theoretical value, in which case the prominent reason is the low K of $\frac{1}{2}$ for this $\nu p_{3/2} \frac{1}{2}^-$ [521] configuration. If an adjustment in the $\frac{7}{2}^- \rightarrow \frac{5}{2}^-$ $M1$ matrix element due to the large signature splitting is taken into account, by including the

TABLE II. Experimental and theoretical ^{185}Pt $B(M1)/B(E2)$ ratios.

Rotational band(s)	Experimental $B(M1)/B(E2)$	Quasiparticle configuration	Theoretical $B(M1)/B(E2)$
1,2 (low spin) ^a	0.25(1)	$\nu i_{13/2}$	0.32
1,2 (high spin) ^b	0.96(11)	$\nu i_{13/2} \otimes (\pi h_{9/2})^2$	0.75
		$(\nu i_{13/2})^3$	0.24
3,4 ^c	0.51(6)	$\nu f_{7/2}$	0.76
		$\nu h_{9/2}$	0.031
5 ^d	0.0021(6) ^d	$\nu p_{3/2}$	0.042
	0.0017(9) ^e		0.0012 ^f
6,7 ^g	1.12(8)	$\nu i_{13/2} \otimes \pi h_{9/2} \otimes \pi i_{13/2}$	1.10
		$\nu i_{13/2} \otimes \pi h_{7/2} \otimes \pi i_{13/2}$	1.65
		$\nu f_{7/2} \otimes (\nu i_{13/2})^2$	0.33
		$\nu p_{3/2} \otimes (\nu i_{13/2})^2$	0.03
		$\nu f_{7/2} \otimes (\pi h_{9/2})^2$	0.82
		$\nu p_{3/2} \otimes (\pi h_{9/2})^2$	0.05

^aAverage for $I = \frac{25}{2} - \frac{31}{2}$.

^bAverage for $\frac{39}{2} - \frac{47}{2}$.

^c $I = \frac{11}{2}$.

^d $I = \frac{7}{2}$, using radioactive decay data of Ref. 15.

^e $I = \frac{7}{2}$, ^{183}Os data of Ref. 22.

^fEffect of signature splitting included.

^g $I = \frac{39}{2}$.

$(1 - \Delta e' / \hbar\omega)^2$ multiplicative factor,²⁷ the agreement between theory and experiment is improved.

Table II lists theoretical $B(M1)/B(E2)$ values for a number of possible three-quasiparticle configurations having negative parity. In the first two cases the $B(M1)$ has been calculated in the so-called “strong-coupling” limit, in which we have included terms depending on the K quantum numbers for all three quasiparticles involved. This is in contrast to the configurations involving a rotation-aligned pair of quasiparticles, in which cases the pair makes no contribution to the magnetic moment component along the symmetry z axis. For bands 6 and 7 the proposed $\nu i_{13/2} \otimes \pi h_{9/2} \otimes \pi i_{13/2}$ coupling is clearly in the best agreement with experiment. As indicated earlier, only a neutron plus two proton combination is capable of producing an $M1$ matrix element large enough to match the data. A possible $\nu f_{7/2} \otimes (\pi h_{9/2})^2$ configuration would undoubtedly be connected with $\nu f_{7/2}$ bands 3 and 4 rather than feed into bands 1 and 2, and would also have an alignment of only $\approx 7.5\hbar$. The mixed $\nu i_{13/2} \otimes \pi f_{7/2} \otimes \pi i_{13/2}$ combination has a very high ratio of transition matrix elements, although it would have about the right amount of alignment. However, as discussed in the preceding section, by analogy with ¹⁸⁴Pt such a configuration is much less likely than an $i_{13/2}$ neutron coupled to the $\pi h_{9/2} \otimes \pi i_{13/2}$ combination.

C. Band crossings

Woods-Saxon cranked shell model calculations, described in Ref. 29, predict possible band crossings due to the rotational alignment either of $i_{13/2}$ neutrons or of $h_{9/2}$ protons. In order of expected frequency, at a defor-

mation of $\beta_2 = 0.22$ and $\gamma = -9^\circ$, they are the $\nu i_{13/2}$ “ AB ” ($\hbar\omega = 0.26$ MeV), $\nu i_{13/2}$ “ BC, AD ” ($\hbar\omega = 0.3$ MeV), and $\pi h_{9/2}$ “ ef ” ($\hbar\omega = 0.36$ MeV) crossings. The labels C and D refer to the second-lowest pair of $\nu i_{13/2}$ quasiparticles, originating from the $\frac{7}{2}^+$ [633] orbital. As shown in Fig. 3, the yrast bands 1 and 2 in ¹⁸⁵Pt experience a gain in alignment of $\approx 5\hbar$ at a frequency of 0.24 MeV. Notwithstanding the theoretical predictions, we believe that the crossing in bands 1 and 2 is most likely caused by a pair of $h_{9/2}$ protons aligning at a surprisingly low frequency. The arguments are as follows.

In ¹⁸⁴Pt one observes²⁶ a double crossing $(\nu i_{13/2})^2(\pi h_{9/2})^2$ with an overall gain in alignment of $\approx 10\hbar$, at an almost degenerate frequency of $\hbar\omega = 0.25$ MeV. In the $\frac{9}{2}^+$ [624] bands (A and B configurations) of ¹⁸⁵Pt the first neutron AB crossing should be blocked, leaving the proton crossing as the logical possibility. However, in this mass region neutron and proton configurations can influence the nuclear deformation in different ways. These shape polarizations in turn can induce significant crossing frequency displacements, which considerably weaken the standard blocking arguments. To illustrate the softness in the γ deformation, the total Routhian surface (TRS) calculations³⁰ for the ¹⁸⁵Pt yrast configuration at a rotational frequencies of 0.25 and 0.30 MeV have been reproduced in Fig. 4. At 0.25 MeV the minimum occurs for $\gamma = -8^\circ$ (slightly triaxial) due to the $i_{13/2}$ quasineutron. At $\hbar\omega = 0.30$ MeV the surface is now distorted significantly towards positive γ by the three-quasiparticle configuration $\nu i_{13/2}(\pi h_{9/2})^2$. In addition, the $(\nu i_{13/2})^3$ minimum can be seen at negative γ , caused by the secondary $\nu i_{13/2}$ BC, AD crossing.

The $B(M1)/B(E2)$ measurements make a more com-

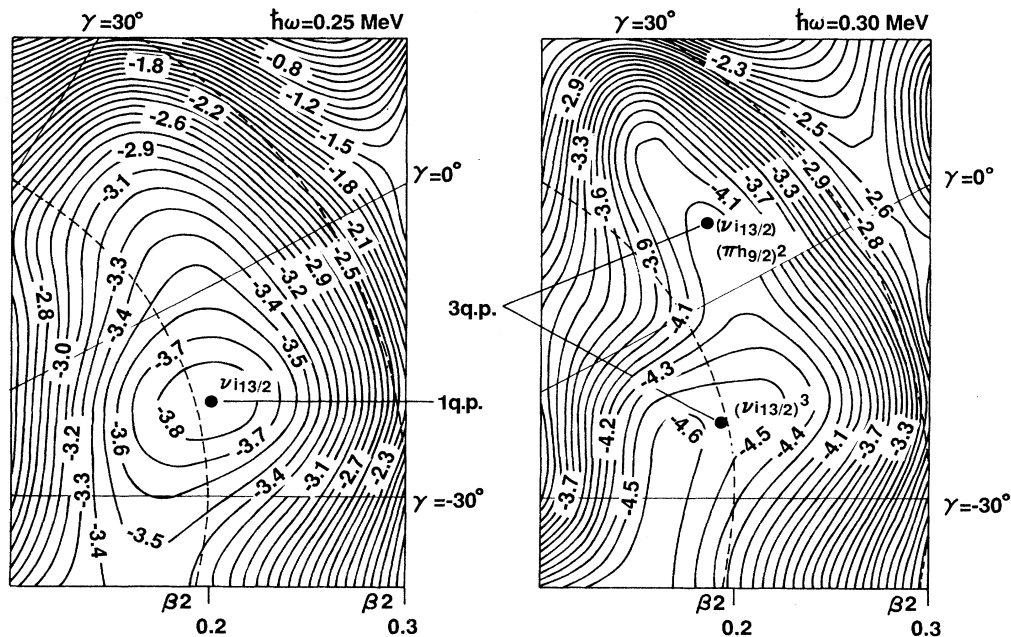


FIG. 4. Total Routhian surface (TRS) calculations for the ¹⁸⁵Pt yrast positive-parity configuration performed at the rotational frequencies, $\hbar\omega$, equal to 0.25 and 0.3 MeV.

elling argument. An observed rise in this ratio by a factor of 3–4 after the upbend strongly suggests a proton crossing,²⁹ especially since an alternative neutron alignment would have an effect in just the opposite direction.

Bands 3 and 4 also show a crossing at $\hbar\omega=0.23$ MeV. At the limit of the data an alignment gain of $\approx 5.5\hbar$ has already occurred, with the end of the crossing not yet in sight. Therefore it is possible that two nearly degenerate crossings are occurring in these bands, similar to the yrast case in ^{184}Pt . Additional data are needed to extend bands 3 and 4 to higher frequencies, though, before the nature of this band crossing (or crossings) can be ascertained.

Band 5, the $vp_{3/2}$ G configuration, reveals a crossing at an identical frequency with an overall gain in alignment of $\approx 6\hbar$. In this case it appears that up to 0.28 MeV in frequency only one alignment process has occurred. The crossings in bands 3, 4, and 5 occur at slightly lower frequencies than does the probable $\pi h_{9/2}$ crossing in bands 1 and 2. It is possible that the $f_{7/2}$ and $p_{3/2}$ bands experience the expected $vi_{13/2}$ AB alignment, which either prevents or delays the competing $\pi h_{9/2}$ ef alignment. Such an effect is possible because the $vi_{13/2}$ band crossing should drive strongly towards negative γ deformation, as shown in Fig. 4, away from the region in γ most favorable to a $\pi h_{9/2}$ crossing.

Bands 6 and 7 show no sign of alignment gain through the band crossing frequency range. This is to be expected, since their Aea, Bea configuration blocks both the neutron AB and proton ef crossings. A secondary $vi_{13/2}$ BC, AD alignment is less likely here than in the yrast A, B bands since the $ea \pi h_{9/2} \otimes \pi i_{13/2}$ combination should drive the nucleus strongly towards positive γ deformation, a trend similar to the $\pi h_{9/2}$ driving tendency shown in Fig. 4.

Normally one would expect bands 6 and 7 to display

the same moderate A, B signature splitting as the yrast bands. However, the signature splitting for the $K=\frac{9}{2}$ $vi_{13/2}$ orbital is even more sensitive to changes in γ deformation than the band crossing frequencies (cf. Ref. 31). In theory a swing to $\gamma \geq 10^\circ$ as shown in Fig. 4 effectively eliminates any energy difference between the two signatures, consistent with the data shown in Fig. 3.

IV. CONCLUSION

The structure of high-spin states in ^{185}Pt has been determined by the $^{173}\text{Yb}(^{16}\text{O}, 4n)$ reaction at 90 MeV using a multidetector array. Rotational bands based on the $\frac{9}{2}^+$ [624], $\frac{7}{2}^-$ [503], and $\frac{1}{2}^-$ [521] neutron orbitals have been identified. An anomalously low proton crossing frequency is implied for the yrast $\frac{9}{2}^+$ [624] bands. Additional work is required to explain the nature of the crossings observed in the $\frac{7}{2}^-$ [503] and $\frac{1}{2}^-$ [521] bands. It has been shown that the semiclassical formalism of Dönau and Frauendorf explains the observed one- and three-quasiparticle configurations reasonably well. Although many aspects of the observed rotational band characteristics are well described by the cranked shell model, more detailed calculations on the effects of alignments on the shape of the γ -soft nucleus ^{185}Pt are clearly needed.

ACKNOWLEDGMENTS

Research at the Université de Montréal and at McMaster University was supported by the Canadian Natural Sciences and Engineering Research Council. Research at the University of Tennessee was supported by the U.S. Department of Energy under Contract DE-SG05-87ER40361. Helpful discussions with F. Dönau regarding the $B(M1)/B(E2)$ calculations are gratefully acknowledged.

*Present address: Argonne National Laboratory, Argonne, IL 60439.

†Present address: Chalk River Nuclear Laboratories, Atomic Energy of Canada Limited, Chalk River, Ontario, Canada K0J 1J0.

‡Present address: Department of Nuclear Physics, Research School of Physical Sciences, Australian National University, Canberra, ACT 2601, Australia.

¹K. Kumar, Phys. Rev. C **1**, 369 (1970).

²M. Cailliau, J. Letessier, H. Flocard, and P. Quentin, Phys. Lett. **46B**, 11 (1973).

³A. Faessler, U. Götz, B. Slavov, and T. Ledergerber, Phys. Lett. **39B**, 579 (1972).

⁴S. Frauendorf and V. Pashkevich, Phys. Lett. **55B**, 365 (1975).

⁵F. Dickman and K. Dietrich, Z. Phys. **263**, 211 (1973).

⁶N. Redon, J. Meyer, M. Meyer, P. Quentin, M. S. Weiss, P. Bonche, H. Flocard, and P.-H. Heenen, Phys. Lett. **B 181**, 223 (1986).

⁷K. Heyde, P. Van Isacker, M. Waroquier, J. L. Wood, and R. A. Meyer, Phys. Rep. **102**, 291 (1983), and references therein.

⁸R. Bengtsson, T. Bengtsson, J. Dudek, G. Leander, W. Na-

zarewicz, and J. Zhang, Phys. Lett. **B 183**, 1 (1987), and references therein.

⁹H. Hubel, A. P. Byrne, S. Oyaga, A. C. Stuchberry, G. D. Dracoulis, and M. Guttormsen, Nucl. Phys. **A453**, 316 (1986).

¹⁰F. Hannachi, G. Bastin, M. G. Porquet, C. Schück, J. P. Thibaud, C. Bourgeois, L. Hildingsson, D. Jerrestam, N. Perrin, H. Sergolle, F. A. Beck, T. Byrski, J. C. Merdinger, and J. Dudek, Nucl. Phys. **A481**, 135 (1988), and references therein.

¹¹A. J. Larabee, M. P. Carpenter, L. L. Riedinger, L. H. Courtney, J. C. Waddington, V. P. Janzen, W. Nazarewicz, J.-Y. Zhang, R. Bengtsson, and G. A. Leander, Phys. Lett. **169B**, 21 (1986).

¹²G. Hebbinghaus, W. Gast, A. Krämer-Flecken, R. M. Lieder, J. Skalski, and W. Urban, Z. Phys. A **328**, 387 (1987).

¹³M. Finger, R. Foucher, J. P. Husson, J. Jastrzebski, A. Johnson, G. Astner, B. R. Erdal, A. Kjelberg, P. Patzelt, A. Høglund, S. G. Malmkog, and R. Henck, Nucl. Phys. **A188**, 369 (1972).

¹⁴B. E. Gnade, R. W. Fink, and J. L. Wood, Nucl. Phys. **A406**, 29 (1983).

¹⁵B. Roussièrè, C. Bourgeois, P. Kilcher, J. Sauvage, M. G. Por-

- quet, and the ISOCELE collaboration, Nucl. Phys. **A438**, 93 (1985).
- ¹⁶M. Piiparinen, J. C. Cunnane, P. J. Daly, C. L. Dors, F. M. Bernthal, and T. L. Khoo, Phys. Lett. **34B**, 1110 (1975).
- ¹⁷G. D. Dracoulis, A. E. Stuchberry, A. P. Byrne, A. R. Poletti, and S. J. Poletti, J. Phys. G **12**, 97 (1986).
- ¹⁸M. A. Deleplanque, C. Gershel, M. Masayasu, N. Perrin, and B. Ader, C. R. Acad. Sci. Ser. B **t.280**, 515 (1975).
- ¹⁹J. T. Routti and S. G. Prussin, Nucl. Instrum. Methods **72**, 125 (1969).
- ²⁰Y. El Masri, thèse de Doctorat, Université de Louvain, 1974.
- ²¹H. J. Rose and P. M. Brink, Rev. Mod. Phys. **39**, 360 (1967).
- ²²B. Roussière, C. Bourgeois, P. Kilcher, J. Sauvage, M. G. Porquet, and A. Wojtasiewicz, Nucl. Phys. **A485**, 111 (1988).
- ²³J. Nyberg *et al.* (unpublished).
- ²⁴R. Bengtsson, S. Frauendorf, and F.-R. May, At. Nucl. Data Tables **35**, 15 (1986).
- ²⁵J. K. Johansson, M.S. thesis, McMaster University, 1987; J. K. Johansson *et al.* (unpublished).
- ²⁶M. P. Carpenter, Ph.D. thesis, University of Tennessee, 1988; M. P. Carpenter *et al.* (unpublished).
- ²⁷F. Dönau, Nucl. Phys. **A471**, 469 (1987).
- ²⁸F. Dönau and S. Frauendorf, in *Proceedings of the Conference on High Angular Momentum Properties of Nuclei, Oak Ridge, 1982*, edited by N. R. Johnson (Harwood Academic, New York, 1983), p. 143.
- ²⁹V. P. Janzen, M. P. Carpenter, L. L. Riedinger, W. Schmitz, S. Pilotte, S. Monaro, D. D. Rajnauth, J. K. Johansson, D. G. Popescu, J. C. Waddington, Y. S. Chen, F. Dönau, and P. B. Semmes, Phys. Rev. Lett. **61**, 2073 (1988).
- ³⁰W. Nazarewicz, J.-Y. Zhang, R. Bengtsson, G. Leander, M. P. Carpenter, V. P. Janzen, L. L. Riedinger, and G. Zhang, Oak Ridge National Laboratory Physics Division Progress Report No. 85, 1986 (unpublished); W. Nazarewicz *et al.* (Knoxville-Lund-Warsaw collaboration) (unpublished).
- ³¹G. Leander, S. Frauendorf, and F.-R. May, in *Proceedings of the Conference on High Angular Momentum Properties of Nuclei, Oak Ridge, 1982*, edited by N. R. Johnson (Harwood Academic, New York, 1983), p. 281.